Non-Gaussian variational approach to Fermi polarons in one- and two-dimensional lattices

Ruijin Liu,[1] Yue-Ran Shi,[1] and Wei Zhang[1,2,*]

[1]*Department of Physics, Renmin University of China, Beijing 100872, China*

[2]*Beijing Key Laboratory of Opto-electronic Functional Materials and Micro-nano Devices, Renmin University of China, Beijing 100872, China*

(Received 22 February 2020; revised 29 July 2020; accepted 6 August 2020; published 2 September 2020)

We study the Fermi polaron problem of one mobile spin-up impurity immersed atop the bath consisting of spin-down fermions in one- and two-dimensional square lattices. We solve this problem by applying a variational approach with non-Gaussian states after separating the impurity and the background via the Lee-Low-Pines transformation. The ground state with a fixed total momentum can be obtained via imaginary-time evolution. For the one-dimensional case, the variational ground-state energy is compared with exact Bethe ansatz solutions and numerical density matrix renormalization-group results with excellent agreement. In two-dimensional lattices, we focus on the dilute limit, and find a polaron-molecule evolution consistent with previous results obtained by variational and quantum Monte Carlo methods for models in continuum space. Compared to previous works, our method provides the lowest ground-state energy in the entire parameter region considered, and has an apparent advantage as it does not need to assume *a priori* any specific form of the variational wave function.

DOI: 10.1103/PhysRevA.102.033305

I. INTRODUCTION

A polaron is defined as a dressed state formed by a mobile impurity interacting with a medium. First proposed by Landau [1] and Pekar [2] more than half a century ago to describe the dressing effect of an impurity by the elementary excitations of the medium, the concept of polaron has attracted great attention and has become a fundamental problem in condensed-matter physics, mainly because it plays an essential role as a building block to understand more complex many-body phenomena [3–5]. Depending on whether the host particle excitations obey Bose or Fermi statistics, a polaron can be classified as a Bose polaron or a Fermi polaron. As the Bose polaron was extensively studied in the context of electron-phonon systems, a Fermi polaron is suggested to behave quite differently since the impurity may undergo a polaron-molecule transition and effectively change its statistics by binding fermions from the background.

In recent years, there has been a significant amount of theoretical work aimed at understanding polaron problems with a variety of tools, such as the variational approach [6] based on Feynman path-integral formalism [7], numerical simulation based upon diagrammatic quantum Monte Carlo method [8–11], and systematic perturbation expansion [12,13] with the use of a T matrix [14–17]. Chevy has provided an instructive variational wave function [18] that captures the essential properties of a polaron, even on a quantitative level when compared with Monte Carlo calculations. This method can be improved by including more particle-hole pair excitations [19–21]. Specifically, by including one and two particle-hole pairs in the variational ansatz, a polaron-molecule transition in a two-dimensional (2D) Fermi gas was obtained [20,21], which agrees well with the experimental results [22].

Ultracold-atomic gases with high controllability provide us with a particularly clean and flexible platform to explore polaron physics. With the aid of Feshbach resonance and optical lattice techniques, polaron properties can be studied to great precision across a broad interaction regime, from attractive to repulsive interaction, in different dimensions. A Fermi polaron was experimentally observed and investigated in highly polarized two-component Fermi gases [23–27]. The observation of Bose polarons has been reported by radio-frequency spectroscopy of bosonic ^{39}K atoms [28] and of ^{40}K impurities in an ultracold bath of ^{87}Rb atoms [29]. In addition, polarons in a 2D Fermi gas involving spin-orbit coupling was theoretically studied [30], which may give rise to a novel Fulde-Ferrell-Larkin-Ovchinnikov-like molecular state. Polaron problems in alkaline-earth(-like) atoms with orbital Feshbach resonance [31–33], in one-dimensional harmonic traps [34,35], and at finite temperatures [36] were also discussed theoretically.

In this paper, we consider a highly polarized Fermi Hubbard model with a single spin-up fermion acting as an impurity interacting with a bath consisting of spin-down fermions. We use the non-Gaussian variational method [37], which for our case can be understood as a combination of the Lee-Low-Pines (LLP) transformation [38] and the Gaussian state approximation, to determine the ground state of the system. Specifically, under the LLP transformation, the impurity degrees of freedom can be eliminated and we can obtain a transformed Hamiltonian describing a single-component system with host spin-down fermions only. Then we use a Gaussian wave function to approximate the transformed ground state and determine the corresponding variational parameters by imaginary-time evolution. We benchmark our results by comparing to the exact Bethe ansatz solution [39] and variational density matrix renormalization-group (DMRG) results [40] for one-dimensional (1D) lattices. For 2D cases, we focus on

*wzhangl@ruc.edu.cn

the dilute limit, which is closely related to continuum systems. By varying the interaction strength, we find a fairly broad region for the system to evolve from polaron to molecule states. The region of evolution is consistent with the results obtained by a Chevy-type variational ansatz [21], diagrammatic Monte Carlo simulation [10,11], and the impurity lattice Monte Carlo method [41]. We emphasize that our approach offers the lowest ground-state energy within the entire region of interaction strength considered, and does not require any knowledge about the wave-function ansatz or any expensive numerical effort. In addition, as our method does not rely on the dimensionality or specific form of the lattice, it can be straightforwardly generalized to other lattice configurations in various dimensions.

The remainder of this manuscript is organized as follows. In Sec. II, we present the polaron problem and employ the LLP transformation to decouple the impurity degree of freedom from the background. By assuming a Gaussian state as the trial wave function for the transformed single-component Hamiltonian, the ground state of the original model takes the form of a non-Gaussian state by adding back the impurity degree of freedom and reversing the LLP transformation, as shown in Sec. III. A numerical minimization of energy is then applied to find the approximate eigenstate for a given total momentum. In Sec. IV, we study a 1D lattice and benchmark the outcome of the non-Gaussian variational approach by the DMRG and Bethe ansatz methods, while the results for a 2D square lattice in the dilute limit are discussed in Sec. V. Finally, we summarize the main conclusion in Sec. VI.

II. HAMILTONIAN AND LEE-LOW-PINES TRANSFORMATION

We consider a Hubbard model for a two-component Fermi system interacting via an on-site interaction on a one-dimensional chain or a two-dimensional square lattice. The lattice spacing $a = 1$ is taken as the length unit throughout this manuscript. The Hamiltonian reads

$$H = -t \sum_{\langle \mathbf{ij}\rangle,\sigma} c^\dagger_{\mathbf{i}\sigma} c_{\mathbf{j}\sigma} + g \sum_{\mathbf{i}} n_{\mathbf{i}\uparrow} n_{\mathbf{i}\downarrow} - \mu \sum_{\mathbf{i}} c^\dagger_{\mathbf{i}\downarrow} c_{\mathbf{i}\downarrow}, \quad (1)$$

where $c^\dagger_{\mathbf{i}\sigma}$ and $c_{\mathbf{i}\sigma}$ are, respectively, creation and annihilation operators for fermions on site $\mathbf{i}$ with spin $\sigma = \uparrow, \downarrow$, $n_{i\sigma} = c^\dagger_{\mathbf{i}\sigma} c_{\mathbf{i}\sigma}$ is the number operator, μ is the chemical potential to tune the number of spin-down particles, and the summation in the first term runs over all nearest-neighboring sites $\langle \mathbf{ij}\rangle$. To study the polaron physics, we focus on the highly polarized limit with only one single spin-up impurity, i.e., $N_\uparrow = \sum_{\mathbf{i}} n_{\mathbf{i}\uparrow} = 1$.

Notice that the system possesses translational symmetry and the total momentum is a good quantum number. To eliminate the impurity degree of freedom, we introduce a unitary transformation,

$$U_{\mathrm{LLP}} = e^{-i\mathbf{Q}\cdot\mathbf{X}}, \quad (2)$$

where $\mathbf{Q} = \sum_{\mathbf{k}} \mathbf{k} c^\dagger_{\mathbf{k}\downarrow} c_{\mathbf{k}\downarrow}$ is the total momentum operator of the spin-down background, $\mathbf{k}$ is the reciprocal lattice vector, and $\mathbf{X} = \sum_{\mathbf{i}} \mathbf{i} c^\dagger_{\mathbf{i}\uparrow} c_{\mathbf{i}\uparrow}$ is the coordinate operator of the spin-up impurity. The transformation given by Eq. (2), known as the Lee-Low-Pines (LLP) transformation, was introduced in 1953 to study the problem of an impurity fermion immersed in a background of phonons [38]. In the following discussion, we show that the same transformation can separate the degrees of freedom of the spin-up impurity and the spin-down Fermi sea, as it does in a Bose medium of phonons. Recently, the LLP transformation was employed to study the Fermi polaron problem in a 1D continuum model [42].

We first rewrite the spin-down part of the Hamiltonian given by Eq. (1) in momentum space,

$$H = -t \sum_{\langle \mathbf{ij}\rangle} c^\dagger_{\mathbf{i}\uparrow} c_{\mathbf{j}\uparrow} + \sum_{\mathbf{k}} (\varepsilon_{\mathbf{k}} - \mu) c^\dagger_{\mathbf{k}\downarrow} c_{\mathbf{k}\downarrow} + \frac{g}{\Omega} \sum_{\mathbf{i},\mathbf{k},\mathbf{k}'} c^\dagger_{\mathbf{i}\uparrow} c_{\mathbf{i}\uparrow} e^{i(\mathbf{k}'-\mathbf{k})\cdot\mathbf{i}} c^\dagger_{\mathbf{k}\downarrow} c_{\mathbf{k}'\downarrow}, \quad (3)$$

where $c_{\mathbf{k}\downarrow} = \frac{1}{\sqrt{\Omega}} \sum_{\mathbf{i}} e^{-i\mathbf{k}\cdot\mathbf{i}} c_{\mathbf{i}\downarrow}$ and $c^\dagger_{\mathbf{k}\downarrow} = \frac{1}{\sqrt{\Omega}} \sum_{\mathbf{i}} e^{i\mathbf{k}\cdot\mathbf{i}} c^\dagger_{\mathbf{i}\downarrow}$ are the fermion operators in momentum space with Ω the number of lattice sites, and the dispersion reads $\varepsilon_{\mathbf{k}} = -2t \cos k$ and $\varepsilon_{\mathbf{k}} = -2t(\cos k_x + \cos k_y)$ for 1D and 2D lattices, respectively. Next, we apply the LLP transformation to Eq. (3). Using the Baker-Campbell-Hausdorff (BCH) formula, the fermion operators $c_{\mathbf{k}\downarrow}$ and $c_{\mathbf{i}\uparrow}$ transform as $U^\dagger_{\mathrm{LLP}} c_{\mathbf{k}\downarrow} U_{\mathrm{LLP}} = e^{-i\mathbf{k}\cdot\mathbf{X}} c_{\mathbf{k}\downarrow}$ and $U^\dagger_{\mathrm{LLP}} c_{\mathbf{i}\uparrow} U_{\mathrm{LLP}} = e^{-i\mathbf{Q}\cdot\mathbf{i}} c_{\mathbf{i}\uparrow}$, respectively. The Hamiltonian after the LLP transformation then takes the following form:

$$H_{\mathrm{LLP}} = \sum_{\mathbf{k}} c^\dagger_{\mathbf{k}\uparrow} c_{\mathbf{k}\uparrow} \left[-t \sum_{\boldsymbol{\delta}} e^{-i(\mathbf{k}-\mathbf{Q})\cdot\boldsymbol{\delta}} \right] + \sum_{\mathbf{k}} (\varepsilon_{\mathbf{k}} - \mu) c^\dagger_{\mathbf{k}\downarrow} c_{\mathbf{k}\downarrow} + \sum_{\mathbf{k}'} c^\dagger_{\mathbf{k}'\uparrow} c_{\mathbf{k}'\uparrow} \left[\frac{g}{\Omega} \sum_{\mathbf{k},\mathbf{q}} c^\dagger_{\mathbf{k}\downarrow} c_{\mathbf{q}\downarrow} \right]. \quad (4)$$

Here, $\boldsymbol{\delta}$ represents the unit lattice vectors, with $\boldsymbol{\delta} = \pm 1$ for 1D and $\boldsymbol{\delta} \in \{(\pm 1, 0), (0, \pm 1)\}$ for 2D lattices. It can be seen that the LLP transformation explicitly separates the total conserved momentum of the system. Indeed, the total conserved momentum is transformed as the momentum of the spin-up particle, which, for a given total momentum, eliminates the degree of freedom of the impurity. Specifically, the momentum of the spin-down atoms transforms as

$$U^\dagger_{\mathrm{LLP}} \sum_{\mathbf{k}} \mathbf{k} c^\dagger_{\mathbf{k}\downarrow} c_{\mathbf{k}\downarrow} U_{\mathrm{LLP}} = \sum_{\mathbf{k}} \mathbf{k} c^\dagger_{\mathbf{k}\downarrow} c_{\mathbf{k}\downarrow}. \quad (5)$$

The momentum of the spin-up impurity transforms as

$$\begin{aligned} U^\dagger_{\mathrm{LLP}} \sum_{\mathbf{k}} \mathbf{k} c^\dagger_{\mathbf{k}\uparrow} c_{\mathbf{k}\uparrow} U_{\mathrm{LLP}} &= \sum_{\mathbf{k}} \sum_{\mathbf{j},\mathbf{j}'} \mathbf{k} e^{i(\mathbf{k}+\mathbf{Q})(\mathbf{j}-\mathbf{j}')} c^\dagger_{\mathbf{j}\uparrow} c_{\mathbf{j}'\uparrow} \\ &= \sum_{\mathbf{k}} \sum_{\mathbf{j},\mathbf{j}'} (\mathbf{k}-\mathbf{Q}) e^{i\mathbf{k}(\mathbf{j}-\mathbf{j}')} c^\dagger_{\mathbf{j}\uparrow} c_{\mathbf{j}'\uparrow} \\ &= \sum_{\mathbf{k}} (\mathbf{k}-\mathbf{Q}) c^\dagger_{\mathbf{k}\uparrow} c_{\mathbf{k}\uparrow} \\ &= \sum_{\mathbf{k}} \mathbf{k} c^\dagger_{\mathbf{k}\uparrow} c_{\mathbf{k}\uparrow} - \mathbf{Q}. \end{aligned} \quad (6)$$

The total momentum of the system transforms as

$$U^\dagger_{\mathrm{LLP}} \sum_{\mathbf{k}} \mathbf{k} (c^\dagger_{\mathbf{k}\uparrow} c_{\mathbf{k}\uparrow} + c^\dagger_{\mathbf{k}\downarrow} c_{\mathbf{k}\downarrow}) U_{\mathrm{LLP}} = \sum_{\mathbf{k}} \mathbf{k} c^\dagger_{\mathbf{k}\uparrow} c_{\mathbf{k}\uparrow}. \quad (7)$$

From Eqs. (5)–(7), we can see that the conserved total momentum of the original model is transformed to the momentum of the impurity. Thus, for a given total momentum $\mathbf{K}$, the ground state of H_{LLP} takes the form $c^\dagger_{\mathbf{K}\uparrow}|0\rangle \otimes |\Psi\rangle_\downarrow$, where $|\Psi\rangle_\downarrow$ is the ground state of the spin-down atoms. By combining with the condition $\sum_{\mathbf{k}} c^\dagger_{\mathbf{k}\uparrow} c_{\mathbf{k}\uparrow} = 1$, Eq. (4) reduces to a Hamiltonian containing a spin-down component only,

$$H_{\mathbf{K}\downarrow} = \sum_{\mathbf{k}} (\varepsilon_{\mathbf{k}} - \mu) c^\dagger_{\mathbf{k}\downarrow} c_{\mathbf{k}\downarrow} + \frac{g}{\Omega} \sum_{\mathbf{k},\mathbf{q}} c^\dagger_{\mathbf{k}\downarrow} c_{\mathbf{q}\downarrow} - t \sum_{\boldsymbol{\delta}} e^{-i(\mathbf{K}-\mathbf{Q})\cdot\boldsymbol{\delta}}. \tag{8}$$

We stress that although the first two terms in Eq. (8) are in a quadratic form of spin-down operators, the third term involves multiscattering processes between particles through the exponential dependence of the operator $\mathbf{Q} = \sum_{\mathbf{k}} \mathbf{k} c^\dagger_{\mathbf{k}\downarrow} c_{\mathbf{k}\downarrow}$. Physically, the Hamiltonian obtained after the LLP transformation describes a polarized medium of spin-down particles with long-range effective interaction mediated by the impurity. The polarization effect of such a strongly correlated many-body system cannot be calculated exactly, and one has to rely on some approximation to obtain the susceptibility.

Next, we construct a variational wave function in a Gaussian form to find the approximate ground state $|\Psi\rangle_\downarrow$ of the Hamiltonian above, and then obtain the eigenstate of the original Hamiltonian with a total conserved momentum by adding back the spin-up impurity and reversing the LLP transformation.

III. NON-GAUSSIAN STATE VARIATIONAL APPROACH

The essence of the variational approach used in this work is to approximate the ground state of Eq. (8) by a Gaussian trial wave function,

$$|\Psi_{\mathrm{GS}}\rangle = U_{\mathrm{GS}}|0\rangle_\downarrow, \tag{9}$$

where the unitary transformation takes the form $U_{\mathrm{GS}} = e^{i\frac{1}{4}A^T\xi_m A}$ for an even particle number of spin-down atoms, or $U_{\mathrm{GS}} = e^{i\frac{1}{4}A^T\xi_m A} a_{1,\mathbf{k}_1}$ for an odd particle number of spin-down atoms, with $A = (a_{1,\mathbf{k}_1}, \ldots, a_{1,\mathbf{k}_\Omega}, a_{2,\mathbf{k}_1}, \ldots, a_{2,\mathbf{k}_\Omega})^T$. The Majorana operators for spin-down fermions are defined as $a_{1,\mathbf{k}_j} = c^\dagger_{\mathbf{k}_j,\downarrow} + c_{\mathbf{k}_j,\downarrow}$ and $a_{2,\mathbf{k}_j} = i(c^\dagger_{\mathbf{k}_j,\downarrow} - c_{\mathbf{k}_j,\downarrow})$, and satisfy the anticommutation relation $\{a_{\alpha,\mathbf{k}}, a_{\beta,\mathbf{k}'}\} = 2\delta_{\alpha\beta}\delta_{\mathbf{k}\mathbf{k}'}$. The variational parameter ξ_m is an antisymmetric Hermitian matrix. To eliminate the gauge degree of freedom in ξ_m, it is convenient to introduce a covariant matrix [37],

$$(\Gamma_m)_{i,j} = \frac{i}{2}\langle\Psi_{\mathrm{GS}}|[A_i, A_j]|\Psi_{\mathrm{GS}}\rangle, \tag{10}$$

where A_i labels the ith element of A. The covariance matrix is related to ξ_m as

$$\Gamma_m = -U_m \Sigma U_m^T, \tag{11}$$

where $U_m = e^{i\xi_m}$ for an even particle number of spin-down atoms and $U_m = e^{i\xi_m} U_v$ for an odd particle number of spin-down atoms,

$$U_v = \begin{pmatrix} 1 & 0 \\ 0 & -\mathbb{1}_{2\Omega-1} \end{pmatrix}, \tag{12}$$

and Σ is constructed by the identity matrix $\mathbb{1}_\Omega$ of dimension Ω as

$$\Sigma \equiv i\sigma_y \otimes \mathbb{1}_\Omega = \begin{pmatrix} 0 & \mathbb{1}_\Omega \\ -\mathbb{1}_\Omega & 0 \end{pmatrix}. \tag{13}$$

The Gaussian variational ansatz given by Eq. (9) represents a mean-field treatment of the correlations among spin-down atoms induced by the third term of the Hamiltonian given by Eq. (8). With the aid of Majorana operators, the state is automatically antisymmetrized, and can be looked upon as an analogy to the Hartree-Fock approximation for electronic gases. In other words, the ansatz given by Eq. (9) describes a screening effect of the spin-down medium onto itself. Thus, by adding back the spin-up impurity and reversing the LLP transformation, the eigenstate of the original Hamiltonian (1) with a total conserved momentum $\mathbf{K}$ can be expressed as a non-Gaussian state,

$$|\Psi_{\mathrm{NGS}}\rangle = U_{\mathrm{LLP}}(c^\dagger_{\mathbf{K}\uparrow} \otimes U_{\mathrm{GS}})|0\rangle. \tag{14}$$

Notice that in such a state, the impurity is scattered off not by a bare spin-down fermion, but by a quasiparticle dressed by other particles. Equivalently, this variational ansatz contains terms of an arbitrary number of particle-hole excitations atop the spin-down Fermi sea, as can be seen in a series expansion of the exponential function of the Gaussian state.

In the spirit of the variational method, the ground state of a Hamiltonian H can be obtained via an imaginary-time evolution of a trial wave function,

$$|\Psi(\tau)\rangle = \frac{e^{-H\tau}|\Psi(0)\rangle}{\sqrt{\langle\Psi(0)|e^{-2H\tau}|\Psi(0)\rangle}}, \tag{15}$$

to the asymptotic limit $\tau \to \infty$ provided that the initial trial state $|\Psi(0)\rangle$ has a nonzero overlap with the ground state. Such an evolution can be described by a differential equation,

$$d_\tau|\Psi(\tau)\rangle = -(H - \langle H\rangle)|\Psi(\tau)\rangle, \tag{16}$$

with the mean energy $\langle H\rangle = \langle\Psi(\tau)|H|\Psi(\tau)\rangle$. Thus, the imaginary-time evolution equation for the non-Gaussian state given by Eq. (14) can be written as

$$d_\tau|\Psi_{\mathrm{NGS}}\rangle = -\mathcal{P}(H - E)|\Psi_{\mathrm{NGS}}\rangle, \tag{17}$$

where $E = \langle\Psi_{\mathrm{NGS}}|H|\Psi_{\mathrm{NGS}}\rangle = \langle\Psi_{\mathrm{GS}}|H_{\mathbf{K}\downarrow}|\Psi_{\mathrm{GS}}\rangle$ is the variational mean energy and $\mathcal{P}$ is the projection operator onto the subspace spanned by tangent vectors of the variational manifold. The left-hand side of Eq. (17) gives

$$d_\tau|\Psi_{\mathrm{NGS}}\rangle = U_{\mathrm{LLP}}[(c^\dagger_{\mathbf{K}\uparrow}|0\rangle_\uparrow) \otimes (U_{\mathrm{GS}}U_L|0\rangle_\downarrow)], \tag{18}$$

where

$$U_L = \frac{1}{4}{:}A^T U_m^T(\partial_\tau U_m)A{:} + \frac{i}{4}\mathrm{Tr}\big[U_m^T(\partial_\tau U_m)\Gamma_m\big], \tag{19}$$

and $:\ :$ represents normal ordering with respect to the vacuum state. The right-hand side of Eq. (17) reads

$$-(H - \langle H\rangle)|\Psi_{\mathrm{NGS}}\rangle = -U_{\mathrm{LLP}}[(c^\dagger_{\mathbf{K}\uparrow}|0\rangle_\uparrow) \otimes (U_{\mathrm{GS}}U_R|0\rangle_\downarrow)], \tag{20}$$

where $U_R = (i/4){:}A^T U_m^T h_m U_m A{:} + \delta H_{\mathbf{K}\downarrow}$. Here, $\delta H_{\mathbf{K}\downarrow}$ denotes the higher-order terms of $c_{k\downarrow}$ that are orthogonal to

the tangential space which will be projected out by $\mathcal{P}$ in Eq. (17), and

$$h_m = 4\frac{\delta E}{\delta \Gamma_m} \tag{21}$$

is the functional derivative of the variational energy. Comparing Eqs. (18) and (20), and combining the covariant parameter defined by Eq. (11), we can finally obtain the imaginary-time equation of motion (EOM) for the covariance matrix Γ_m [37,43],

$$\partial_\tau \Gamma_m = -h_m - \Gamma_m h_m \Gamma_m. \tag{22}$$

To evolve the variational parameter Γ_m according to the EOM given by Eq. (22), we need to calculate the functional derivative h_m defined in Eq. (21). First of all, we calculate the variational energy $E = \langle \Psi_{\rm GS}|H_{\mathbf{K}\downarrow}|\Psi_{\rm GS}\rangle$. Using the relations $c^\dagger_{\mathbf{k},\downarrow} = \frac{1}{2}(a_{1,\mathbf{k}} - ia_{2,\mathbf{k}})$ and $c_{\mathbf{k},\downarrow} = \frac{1}{2}(a_{1,\mathbf{k}} + ia_{2,\mathbf{k}})$, we can rewrite the first two terms of $H_{\mathbf{K}\downarrow}$ in Eq. (8) as

$$\begin{aligned}\sum_{\mathbf{k}}(\varepsilon_{\mathbf{k}} - \mu)c^\dagger_{\mathbf{k}\downarrow}c_{\mathbf{k}\downarrow} + \frac{g}{\Omega}\sum_{\mathbf{k},\mathbf{q}} c^\dagger_{\mathbf{k}\downarrow}c_{\mathbf{q}\downarrow} &= \frac{1}{4}\sum_{\mathbf{k}}(\varepsilon_{\mathbf{k}} - \mu)(a_{1,\mathbf{k}}a_{1,\mathbf{k}} + a_{2,\mathbf{k}}a_{2,\mathbf{k}} - ia_{2,\mathbf{k}}a_{1,\mathbf{k}} + ia_{1,\mathbf{k}}a_{2,\mathbf{k}}) \\ &\quad + \frac{g}{4\Omega}\sum_{\mathbf{k},\mathbf{q}}(a_{1,\mathbf{k}}a_{1,\mathbf{q}} + a_{2,\mathbf{k}}a_{2,\mathbf{q}} - ia_{2,\mathbf{k}}a_{1,\mathbf{q}} + ia_{1,\mathbf{k}}a_{2,\mathbf{q}}) \\ &= \frac{1}{2}\sum_{\mathbf{k}}\left(\varepsilon_{\mathbf{k}} - \mu + \frac{g}{\Omega}\right) + \frac{i}{4}A^T H_0 A - \frac{i\mu}{4}A^T \Sigma A. \end{aligned} \tag{23}$$

The matrix Σ is defined as in Eq. (13), and $H_0 = i\sigma_y \otimes [\mathrm{diag}(\varepsilon_{\mathbf{k}}) + (g/\Omega)J_\Omega]$, where $\mathrm{diag}(\varepsilon_{\mathbf{k}})$ is an $\Omega \times \Omega$ diagonal matrix with diagonal matrix elements $\varepsilon_{\mathbf{k}_1}, \cdots, \varepsilon_{\mathbf{k}_\Omega}$, and J_Ω is an $\Omega \times \Omega$ matrix with all elements being 1. The expectation value of the term $(i/4)A^T H_0 A$ under the Gaussian state can be calculated as

$$\begin{aligned}\frac{i}{4}\langle \Psi_{\rm GS}|A^T H_0 A|\Psi_{\rm GS}\rangle &= \frac{i}{4}\sum_{i,j}(H_0)_{i,j}\langle \Psi_{\rm GS}|A_i A_j|\Psi_{\rm GS}\rangle = \frac{i}{4}\sum_{i<j}[(H_0)_{i,j}\langle \Psi_{\rm GS}|A_i A_j|\Psi_{\rm GS}\rangle + (H_0)_{j,i}\langle \Psi_{\rm GS}|A_j A_i|\Psi_{\rm GS}\rangle] \\ &= \frac{i}{4}\sum_{i<j}(H_0)_{i,j}\langle \Psi_{\rm GS}|([A_i, A_j])|\Psi_{\rm GS}\rangle = \frac{1}{2}\sum_{i<j}(H_0)_{i,j}(\Gamma_m)_{i,j} = \frac{1}{4}\sum_{i,j}(H_0)_{i,j}(\Gamma_m)_{i,j}, \end{aligned} \tag{24}$$

where we have used the antisymmetry of H_0 and the covariance matrix Γ_m defined in Eq. (10). Similarly, we can obtain the following expression:

$$\frac{i\mu}{4}\langle \Psi_{\rm GS}|A^T \Sigma A|\Psi_{\rm GS}\rangle = \frac{\mu}{4}\sum_{i,j}\Sigma_{i,j}(\Gamma_m)_{i,j}. \tag{25}$$

The mean value of the operators that take the form as the third term in Eq. (8) can be obtained by introducing coherent representation for the fermionic Gaussian state, and the result is [37]

$$\langle \Psi_{\rm GS}|e^{i\mathbf{Q}\cdot\boldsymbol{\delta}}|\Psi_{\rm GS}\rangle = \left(-\tfrac{1}{2}\right)^\Omega s_f \mathrm{Pf}(\Gamma_F), \tag{26}$$

where $s_f = (-1)^{\Omega/2}$ and $s_f = (-1)^{(\Omega-1)/2}$ for Ω being even and odd, respectively. Other quantities in the expression above are $\Gamma_F = \sqrt{1 - e^{i\alpha}}\Gamma_m\sqrt{1 - e^{i\alpha}} - (1 + e^{i\alpha})\Sigma$, $\alpha = \mathbb{1}_2 \otimes \mathrm{diag}(\mathbf{k}\cdot\boldsymbol{\delta})$, with $\mathrm{diag}(\mathbf{k}\cdot\boldsymbol{\delta})$ a diagonal matrix with diagonal elements $\mathbf{k}_1\cdot\boldsymbol{\delta}, \ldots, \mathbf{k}_\Omega\cdot\boldsymbol{\delta}$, and $\mathrm{Pf}(\Gamma_F)$ denotes the Pfaffian of Γ_F. Combining Eqs. (24)–(26), we obtain the variational energy

$$\begin{aligned} E &= \langle \Psi_{\rm GS}|H_{\mathbf{K}\downarrow}|\Psi_{\rm GS}\rangle \\ &= \frac{1}{2}\sum_{\mathbf{k}}\varepsilon_{\mathbf{k}} - \frac{\Omega\mu}{2} + \frac{g}{2} + \frac{1}{4}\sum_{i,j}(H_0)_{i,j}(\Gamma_m)_{i,j} \\ &\quad - t\sum_{\boldsymbol{\delta}} e^{-i\mathbf{K}\cdot\boldsymbol{\delta}}\left(-\frac{1}{2}\right)^\Omega s_f \mathrm{Pf}(\Gamma_F) - \frac{\mu}{4}\sum_{i,j}\Sigma_{i,j}(\Gamma_m)_{i,j}. \end{aligned} \tag{27}$$

The functional derivative h_m is

$$\begin{aligned} h_m = H_0 - \mu\Sigma + 2t\sum_{\boldsymbol{\delta}}\Bigg[& e^{-i\mathbf{K}\cdot\boldsymbol{\delta}}\left(-\frac{1}{2}\right)^\Omega \\ & \times s_f \mathrm{Pf}(\Gamma_F)\sqrt{1 - e^{i\alpha}}\Gamma_F^{-1}\sqrt{1 - e^{i\alpha}}\Bigg]. \end{aligned} \tag{28}$$

In addition, the particle number of the spin-down medium is determined by

$$N_\downarrow = -\frac{\partial E}{\partial \mu} = \frac{\Omega}{2} + \frac{1}{4}\sum_{i,j}\Sigma_{i,j}(\Gamma_m)_{i,j}. \tag{29}$$

In the following discussion, we evolve the variational parameter Γ_m via Eqs. (22) and (28) until a convergence of variational

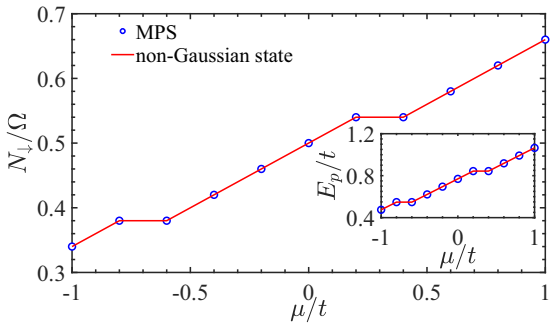

FIG. 1. Particle number of the spin-down component and ground-state energy of a Fermi polaron (inset) in a 1D lattice by varying the chemical potential. Results obtained by the non-Gaussian variational approach and DMRG method with MPS representation reach an excellent agreement. Parameters used in this figure are $g/t = 2$, $\mathbf{K} = 0$, and $\Omega = 50$.

energy given by Eq. (27) is reached under a number constraint given by Eq. (29).

IV. ONE-DIMENSIONAL CASE

First, we focus on the one-dimensional case and study the dispersion of the system for a given total momentum $\mathbf{K}$. In our numerical variation, we evolve the imaginary-time EOM (22) until a convergence to a steady state is reached. To ensure the resulting state is the true ground state, we run the evolution for a set of randomly generated initial states and choose the outcome with lowest energy. The variational results are then compared with those obtained by Bethe ansatz (BA) [39] and the variational DMRG method based on matrix product states (MPS) representation under a periodic boundary condition, with system size $\Omega = 50$, a maximum bond dimension up to $M = 1200$, and a restriction of energy variance less than 10^{-6}.

Figures 1 and 2 show the results of zero total momentum, $\mathbf{K} = 0$. We first point out that the results obtained by the non-Gaussian state with $\mathbf{K} = 0$ agree perfectly well with those obtained by DMRG without specifying the total momentum $\mathbf{K}$, indicating that the ground state has a zero total momentum.

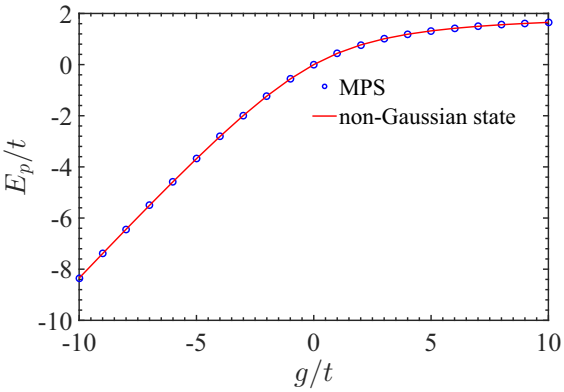

FIG. 2. Ground-state energy of a Fermi polaron in a 1D lattice by varying the interaction strength. Other parameters are taken as $N_\downarrow = 25$, $\mathbf{K} = 0$, and $\Omega = 50$.

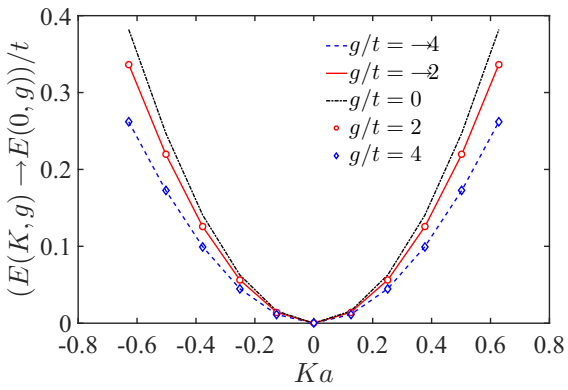

FIG. 3. Dispersion relations for a 1D Fermi polaron with various interaction strengths. Results for the interaction with opposite signs are identical owing to the partial particle-hole symmetry as discussed in the text. The effective mass increases with interaction strength $|g|$, revealing a more significant dressing effect induced by the bath. Other parameters used in this plot are $N_\downarrow = 25$ and $\Omega = 50$.

Owing to the finite-size effect, we observe a steplike jump in both the particle number and the ground-state energy by varying the chemical potential, as depicted in Fig. 1. To further elucidate the interaction effect, in this figure and the following discussion, we set the zero point energy to be the energy of the corresponding noninteracting case, and define the polaron energy as $E_p(\mathbf{K}, g) \equiv E(\mathbf{K}, g) - E(\mathbf{K} = 0, g = 0)$. Notice that the noninteracting system energy $E(\mathbf{K} = 0, g = 0)$ can be calculated exactly.

In Fig. 2, we fix the density of spin-down particles $N_\downarrow/\Omega = 0.5$ and vary the interaction g from attractive to repulsive. This result perfectly matches the BA solution [39], which is not distinguishable from the curve of our non-Gaussian variational data. It can be seen that the ground-state energy varies smoothly versus the interaction. In the limit of infinitely large repulsion $g \to +\infty$, the spin-up impurity acts an effective hard wall for spin-down particles, which cuts two links with hopping rate t and hence leads to an energy $E_p \to 2t$. In the opposite limit of large attractive interaction $g \to -\infty$, the spin-up impurity is tightly bound with one spin-down particle, and acting together as an impenetrable boundary due to the Pauli blocking effect. Thus, the energy tends to the limiting value of $E_p \to g + 2t$. Our numerical results are consistent with the two limits.

Next, we fix the density of spin-down particles at half filling with $\mu = 0$ and $N_\downarrow/\Omega = 0.5$, and extract the dispersion relation $E(\mathbf{K}, g) - E(0, g)$ by varying the total momentum $\mathbf{K}$ with interaction strength $g/t = 0, \pm 2, \pm 4$. From Fig. 3, we find that the effective mass of the quasiparticle defined as

$$m^* = \left(\frac{\partial^2 E}{\partial K^2}\bigg|_{K=0} \right)^{-1} \tag{30}$$

is independent of the sign of the interaction and increases monotonically with $|g|$. The symmetry with respect to the sign of the interaction can be understood by applying a partial particle-hole transformation [44],

$$U_\downarrow \equiv \prod_j [c_{j\downarrow} + (-1)^j c_{j\downarrow}^\dagger], \tag{31}$$

which transforms the operators $c_{i\sigma}$ as

$$U_\downarrow^\dagger c_{i\uparrow} U_\downarrow = c_{i\uparrow}, \quad U_\downarrow^\dagger c_{i\downarrow} U_\downarrow = (-1)^i c_{i\downarrow}^\dagger. \tag{32}$$

At half filling with $\mu = 0$, the Hamiltonian given by Eq. (1) is transformed under Eq. (31) as

$$U_\downarrow^\dagger H(g, \mu = 0) U_\downarrow = H(-g, \mu = 0) + g \sum_i c_{i\uparrow}^\dagger c_{i\uparrow}, \tag{33}$$

while the number constraint remains unchanged, i.e., $N_\uparrow = 1$ and $N_\downarrow/\Omega = 0.5$. Thus, we have the relation of the energy spectra for the interaction of opposite signs,

$$E(\mathbf{K}, g) = E(\mathbf{K}, -g) + g, \tag{34}$$

at half filling. This result shows that the difference between $E(\mathbf{K}, g)$ and $E(\mathbf{K}, -g)$ is a constant g, and the effective masses for the two cases are equivalent.

V. TWO-DIMENSIONAL CASE IN THE DILUTE LIMIT

In this section, we employ the non-Gaussian variational approach to a 2D square lattice. We focus on the dilute limit with the number of spin-down particles that is much smaller than that of the lattice sites, i.e., $N_\downarrow \ll \Omega$. This limit is of particular interest as it is closely related to the continuum model, which can be considered as a lattice model with an infinitesimal lattice spacing, $d \to 0$. The problem of the Fermi polaron in a 2D continuum system has been studied using various methods [10,11,20,21,41]. Previous works using a variational approach by including more pairs of particle-hole excitations show that there exists a polaron-molecule transition in the ground state as the interaction varies [20,21]. Similar findings have been obtained in diagrammatic Monte Carlo (diagMC) simulations [10,11]. All of these variational and diagMC studies perform separate calculations for polaron and molecule states, where the transition is identified as the level crossing point of the two states. Later, in order to study the transition region in a unified way, a fully nonperturbative calculation was performed using the impurity lattice Monte Carlo (ILMC) method [41]. One feature of the ILMC method is the discretization of the spatial part. The results obtained by ILMC show evidence for a smooth crossover from polaron to molecule states. Here, we study the 2D lattice model in the dilute limit via the non-Gaussian variational approach, without assuming *a priori* any specific form of the wave function. In the following calculation, we take the lattice size as $\Omega = 50 \times 50$ and $N_\downarrow \approx 37$, which corresponds to a filling density $N_\downarrow/\Omega \approx 0.0148$. Systems with smaller size and different filling factor are also tested for various interacting strengths to ensure that the finite-size effect is negligible.

In a 2D continuum model, the interaction strength g is characterized by the binding energy E_b of a two-body bound state. To make a quantitative comparison, we first solve for the two-body bound state in the lattice Hamiltonian. In momentum space, the two-body Hamiltonian reads

$$H^{(2)} = \sum_{\mathbf{k},\sigma} \varepsilon'_{\mathbf{k}} c_{\mathbf{k}\sigma}^\dagger c_{\mathbf{k}\sigma} + \frac{g}{\Omega} \sum_{\mathbf{q},\mathbf{k},\mathbf{k}'} c_{\mathbf{q}-\mathbf{k}\uparrow}^\dagger c_{\mathbf{k}\downarrow}^\dagger c_{\mathbf{k}'\downarrow} c_{\mathbf{q}-\mathbf{k}'\uparrow}, \tag{35}$$

with single-particle dispersion

$$\varepsilon'_{\mathbf{k}} = \varepsilon_{\mathbf{k}} + 4 = -2t\cos(k_x) - 2t\cos(k_y) + 4 \tag{36}$$

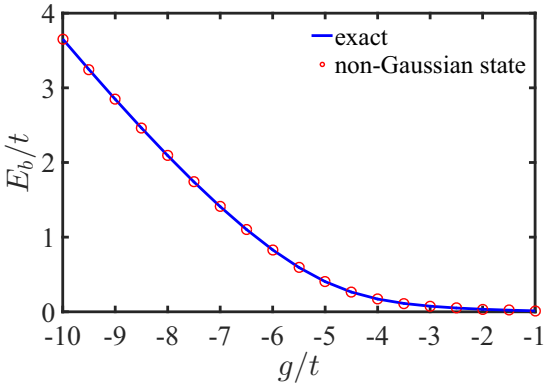

FIG. 4. Two-body bound-state energy for a single spin-up and a single spin-down atom in a 2D square lattice of size 50×50. The exact result is obtained by solving the two-body problem analytically as in Eq. (40).

and number constraints $\sum_{\mathbf{k}} c_{\mathbf{k}\uparrow}^\dagger c_{\mathbf{k}\uparrow} = \sum_{\mathbf{k}} c_{\mathbf{k}\downarrow}^\dagger c_{\mathbf{k}\downarrow} = 1$. Notice that we have shifted the zero-energy point to the band bottom to get a direct comparison with the continuum model. The two-body wave function with zero total momentum can be generally written as

$$|\Psi^{(2)}\rangle = \sum_{\mathbf{k}} \Psi_{\mathbf{k}}^{(2)} c_{\mathbf{k}\uparrow}^\dagger c_{-\mathbf{k}\downarrow}^\dagger |0\rangle. \tag{37}$$

Substituting Eq. (37) into the Schrödinger equation,

$$H^{(2)}|\Psi^{(2)}\rangle = E^{(2)}|\Psi^{(2)}\rangle, \tag{38}$$

we obtain the following equation for the coefficients $\Psi_{\mathbf{k}}^{(2)}$:

$$2\varepsilon'_{\mathbf{k}} \Psi_{\mathbf{k}}^{(2)} + \frac{g}{\Omega} \sum_{\mathbf{k}'} \Psi_{\mathbf{k}'}^{(2)} = E^{(2)} \Psi_{\mathbf{k}}^{(2)}. \tag{39}$$

Equation (39) leads to a self-consistent equation,

$$-\frac{1}{g} = \frac{1}{\Omega} \sum_{\mathbf{k}} \frac{1}{E_b + 2\varepsilon'_{\mathbf{k}}}, \tag{40}$$

where $E_b = -E^{(2)}$ is the two-body binding energy. The two-body ground state of Eq. (35) can also be obtained numerically via the non-Gaussian variational method. In Fig. 4, we show the results of E_b obtained by the two methods and find excellent agreement. This observation is another evidence for the validity of the variational approach.

With the connection between the lattice and continuum models built by Eq. (40), we replace g in the Hamiltonian (1) with E_b, and solve for the ground state with total momentum $\mathbf{K} = 0$. As in the 1D case, we define the polaron energy as the shift induced by the interaction,

$$E_p \equiv E(g) - E(g = 0), \tag{41}$$

and plot the subtracted-scaled polaron energy $(E_p + E_b)/E_f$ versus the dimensionless interaction $\eta \equiv \frac{1}{2}\ln(2E_f/E_b)$ in Fig. 5. Here, the Fermi energy $E_f = \varepsilon'(\mathbf{k}_f)$ is defined via the shifted dispersion relation given by Eq. (36) with Fermi momentum $\mathbf{k}_f$.

From Fig. 5(a), we find that the variational result approaches the value of a noninteraction system in the weak-coupling limit with large positive η, and saturates to the

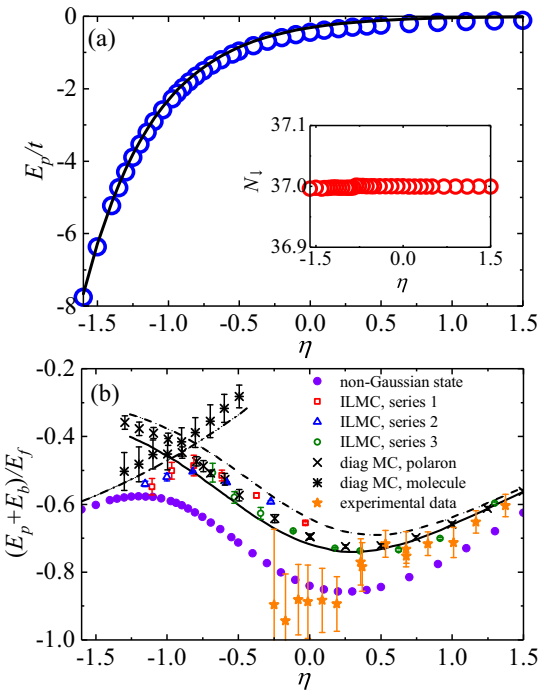

FIG. 5. (a) The non-Gaussian variational ground-state energy (blue circles) of a 2D Fermi polaron with number of background particles $N_\downarrow \approx 37$ (inset) in a square lattice of size 50×50. The system is in the dilute limit with $N_\downarrow/\Omega \approx 0.0148$. The energy saturates to the noninteracting value $E_p = 0$ in the weak-coupling limit with large positive η, and to the two-body bound-state energy $-E_b$ (black solid line) in the strong-coupling limit with large negative η. (b) A polaron-molecule evolution can be observed by plotting the polaron energy in a scaled way. The results are compared with the outcome obtained using the Chevy-like polaron ansatz with one particle-hole pair excitation (dashed line) [20], the same ansatz with two particle-hole pair excitations (solid line) [21], and the molecule variational wave function with one particle-hole excitation pair (dash-dotted line) [20]. Some numerical solutions using diagrammatic quantum Monte Carlo (diagMC) [10] and impurity lattice Monte Carlo (ILMC) [41], as well as the experimental data for highly polarized quasi-two-dimensional Fermi gases [45], are also shown for comparison.

two-body bound-state energy $-E_b$ (solid line) in the strong-coupling limit with large negative η. This observation suggests that the system transforms from a polaron to a molecule state by increasing the interaction from zero. In fact, compared with the energies of polaron and molecule states obtained by either Chevy-like ansatz or diagrammatic MC, as shown in Fig. 5(b), the results obtained by the non-Gaussian variational approach show good agreement in the corresponding weak and strong interacting limits. In the intermediate interaction regime, the non-Gaussian variational method reveals a fairly broad evolution from polaron to molecule states, with a ground-state energy significantly lower than all other numerical and variational methods throughout the entire parameter region. We emphasize that in this calculation, one does not need to assume any specific form of the trial wave function, and the results for different interaction strengths are obtained via the same algorithm with very economical numerical efforts. The numerical convergence is quite stable against different initial states and variational routes. From Fig. 5(b), we estimate that the polaron-molecule evolution takes place within the parameter region $-1.3 < \eta < -1$, which is approximately consistent with those obtained by the Chevy-like ansatz [21] with $-0.97 < \eta < -0.80$, the diagMC method [10] with $-1.1 < \eta < -0.8$, and the ILMC method [41] with $-0.9 < \eta < -0.75$ for 2D systems, as well as the diagMC method with $-1.3 < \eta < -0.9$ for quasi-2D geometries [11].

To extract more information about the evolution between the polaron and molecule states, we calculate the density-density correlation function defined as

$$C_{\uparrow\downarrow}(\mathbf{x}) = \langle \Psi_{\mathrm{NGS}} | c^\dagger_{\mathbf{i}+\mathbf{x},\uparrow} c_{\mathbf{i}+\mathbf{x},\uparrow} c^\dagger_{\mathbf{i},\downarrow} c_{\mathbf{i},\downarrow} | \Psi_{\mathrm{NGS}} \rangle, \tag{42}$$

which can be transformed as mean value problems in the Gaussian state as

$$C_{\uparrow\downarrow}(\mathbf{x}) = \frac{1}{\Omega} \sum_{\mathbf{k},\mathbf{k}'} e^{i(\mathbf{k}-\mathbf{k}')\cdot\mathbf{x}} \langle \Psi_{\mathrm{GS}} | c^\dagger_{\mathbf{k},\downarrow} c_{\mathbf{k}',\downarrow} | \Psi_{\mathrm{GS}} \rangle. \tag{43}$$

From Fig. 6(a), we observe a smooth change of the correlation function by varying the interaction strength η. In the weakly interacting case of $\eta = 0.5$, the distribution of the spin-down background fermions is fairly extended around the impurity, showing a polarization effect of the medium induced by the impurity. As the interaction strength increases, the spin-down particles gradually concentrate on the spot of impurity, and eventually form a tightly bound dimers. The correlation function shows dips around the dimer as a result of the Pauli exclusion principle. When moving further away from the impurity, the correlation approaches the background value of a noninteracting Fermi system. The variation of the correlation function also suggests a smooth crossover from the polaron to molecule states, as previously discussed by the ILMC algorithm [41]. In cold-atom experiments, the real-space density-density correlation can be extracted from *in situ* imaging [46], Bragg spectroscopy [47], or time-of-flight measurements [48,49].

Another quantity of particular interest is the quasiparticle residue defined as

$$Z = |(\langle \mathrm{FS}|_\uparrow \langle 0|c_{k=0,\uparrow})|\Psi_{\mathrm{NGS}}\rangle|^2 = |\langle \mathrm{FS}|\Psi_{\mathrm{GS}}\rangle|^2, \tag{44}$$

where $|\mathrm{FS}\rangle = \prod_{k<=|\mathbf{k}_f|} c^\dagger_{\mathbf{k}\downarrow}|0\rangle$ denotes the noninteracting ground state of the spin-down atoms, i.e., the noninteracting Fermi sea. This quantity reveals to what extent the many-body wave function is modified by the interaction and can be extracted by the radio-frequency spectroscopy [26,50]. According to Eq. (10), the covariant matrix of $|\mathrm{FS}\rangle$ reads

$$\Gamma_{m,\mathrm{FS}} = \begin{pmatrix} 0 & \mathrm{diag}((-1)^{n_{\mathbf{k}\downarrow}+1}) \\ -\mathrm{diag}((-1)^{n_{\mathbf{k}\downarrow}+1}) & 0 \end{pmatrix}, \tag{45}$$

where $n_{\mathbf{k}\downarrow}$ denotes the particle number of the spin-down component with momentum $\mathbf{k}$, and $\mathrm{diag}((-1)^{n_{\mathbf{k}\downarrow}+1})$ is a diagonal matrix with elements $(-1)^{n_{\mathbf{k}_1\downarrow}+1}, \ldots, (-1)^{n_{\mathbf{k}_\Omega\downarrow}+1}$. Thus, the quasiparticle residue here can be viewed as the overlap between two Gaussian states and can be calculated as [51]

$$Z = 2^{-\Omega}\mathrm{Pf}(-\Gamma_{m,\mathrm{FS}})\mathrm{Pf}(-\Gamma_{m,\mathrm{FS}} - \Gamma_m). \tag{46}$$

As shown in Fig. 6(b), the quasiparticle residue decreases monotonically and smoothly from unity to zero as η varies

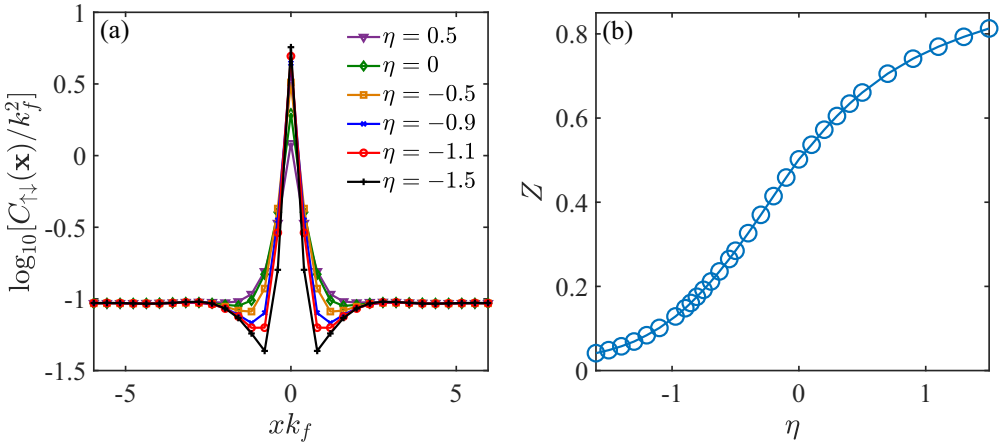

FIG. 6. (a) Density-density correlation function $C_{\uparrow\downarrow}(\mathbf{x})$ and (b) quasiparticle residue of a 2D polaron with the lattice size $\Omega = 50 \times 50$ and the particle number $N_\downarrow \approx 37$. In (a), we take $\mathbf{x} = (x, 0)$, and k_f is the Fermi wave vector along the x direction.

from the weakly to strongly interacting limits, also suggesting a crossover from the polaron to molecule states rather than a phase transition.

VI. CONCLUSION

We study the polaron problem of a Fermi Hubbard model in one- and two-dimensional square lattices. By employing the Lee-Low-Pines transformation to separate the impurity from the background fermions, and the Gaussian approximation for the resulting bath Hamiltonian, we obtain a variational wave function in the form of a non-Gaussian state, where the variational parameters are determined by imaginary-time evolution. For one-dimensional lattices, we calculate the ground-state energy and dispersion relation, and achieve excellent agreement with the Bethe ansatz and DMRG results. For the two-dimensional case, we focus on the dilute limit and find an evolution from the polaron to molecule states by varying the interaction strength, without assuming *a priori* any specific form of the state. The parameter region of the evolution is consistent with the existing results obtained by the variational method, diagrammatic quantum Monte Carlo simulation, and impurity lattice Monte Carlo algorithm. Our results of the ground-state energy, the density-density correlation function, and the quasiparticle residue all suggest a smooth crossover from the polaron to the molecule states. We emphasize that as the present method does not rely on the dimensionality or specific form of the lattice, it can be straightforwardly generalized to other lattice configurations in various dimensions.

ACKNOWLEDGMENTS

This work is supported by the National Natural Science Foundation of China (Grants No. 11434011, No. 11522436, and No. 11774425), the National Key R&D Program of China (Grant No. 2018YFA0306501), the Beijing Natural Science Foundation (Grant No. Z180013), the Joint Fund of the Ministry of Education (Grant No. 6141A020333xx), and the Research Funds of Renmin University of China (Grants No. 16XNLQ03 and No. 18XNLQ15).

[1] L. D. Landau, Phys. Z. Sowjetunion **3**, 664 (1933).
[2] S. I. Pekar, Zh. Eksp. Teor. Fiz. **16**, 341 (1946).
[3] L. D. Landau and S. I. Pekar, Zh. Eksp. Teor. Fiz. **18**, 419 (1948).
[4] J. B. McGuire, J. Math. Phys. **6**, 432 (1965).
[5] J. B. McGuire, J. Math. Phys. **7**, 123 (1966).
[6] J. Tempere, W. Casteels, M. K. Oberthaler, S. Knoop, E. Timmermans, and J. T. Devreese, Phys. Rev. B **80**, 184504 (2009).
[7] R. P. Feynman, Phys. Rev. **97**, 660 (1955).
[8] N. V. Prokof'ev and B. V. Svistunov, Phys. Rev. Lett. **81**, 2514 (1998).
[9] A. S. Mishchenko, N. V. Prokof'ev, A. Sakamoto, and B. V. Svistunov, Phys. Rev. B **62**, 6317 (2000).
[10] J. Vlietinck, J. Ryckebusch, and K. Van Houcke, Phys. Rev. B **89**, 085119 (2014).
[11] P. Kroiss and L. Pollet, Phys. Rev. B **90**, 104510 (2014).
[12] S. P. Rath and R. Schmidt, Phys. Rev. A **88**, 053632 (2013).
[13] R. S. Christensen, J. Levinsen, and G. M. Bruun, Phys. Rev. Lett. **115**, 160401 (2015).
[14] A. L. Fetter, *Quantum Theory of Many-Particle Systems* (McGraw-Hill, New York, 1994).
[15] P. Massignan and G. M. Bruun, Eur. Phys. J. D **65**, 83 (2011).
[16] P. Massignan, Z. Yu, and G. M. Bruun, Phys. Rev. Lett. **110**, 230401 (2013).
[17] R. Combescot, A. Recati, C. Lobo, and F. Chevy, Phys. Rev. Lett. **98**, 180402 (2007).
[18] F. Chevy, Phys. Rev. A **74**, 063628 (2006).
[19] S. Zöllner, G. M. Bruun, and C. J. Pethick, Phys. Rev. A **83**, 021603(R) (2011).
[20] M. M. Parish, Phys. Rev. A **83**, 051603(R) (2011).
[21] M. M. Parish and J. Levinsen, Phys. Rev. A **87**, 033616 (2013).
[22] M. Koschorreck, D. Pertot, E. Vogt, B. Fröhlich, M. Feld, and M. Köhl, Nature (London) **485**, 619 (2012).
[23] M. W. Zwierlein, A. Schirotzek, C. H. Schunck, and W. Ketterle, Science **311**, 492 (2006).

[24] M. W. Zwierlein, C. H. Schunck, A. Schirotzek, and W. Ketterle, Nature (London) **442**, 54 (2006).
[25] G. B. Partridge, W. Li, R. I. Kamar, Y. Liao, and R. G. Hulet, Science **311**, 503 (2006).
[26] A. Schirotzek, C.-H. Wu, A. Sommer, and M. W. Zwierlein, Phys. Rev. Lett. **102**, 230402 (2009).
[27] C. Kohstall, M. Zaccanti, M. Jag, A. Trenkwalder, P. Massignan, G. M. Bruun, F. Schreck, and R. Grimm, Nature (London) **485**, 615 (2012).
[28] N. B. Jørgensen, L. Wacker, K. T. Skalmstang, M. M. Parish, J. Levinsen, R. S. Christensen, G. M. Bruun, and J. J. Arlt, Phys. Rev. Lett. **117**, 055302 (2016).
[29] M.-G. Hu, M. J. Van de Graaff, D. Kedar, J. P. Corson, E. A. Cornell, and D. S. Jin, Phys. Rev. Lett. **117**, 055301 (2016).
[30] W. Yi and W. Zhang, Phys. Rev. Lett. **109**, 140402 (2012).
[31] J.-G. Chen, T.-S. Deng, W. Yi, and W. Zhang, Phys. Rev. A **94**, 053627 (2016).
[32] T.-S. Deng, Z.-C. Lu, Y.-R. Shi, J.-G. Chen, W. Zhang, and W. Yi, Phys. Rev. A **97**, 013635 (2018).
[33] J.-G. Chen, Y.-R. Shi, X. Zhang, and W. Zhang, Front. Phys. **13**, 136702 (2018).
[34] E. V. H. Doggen, A. Korolyuk, P. Törmä, and J. J. Kinnunen, Phys. Rev. A **89**, 053621 (2014).
[35] J. Kwasniok, S. I. Mistakidis, and P. Schmelcher, Phys. Rev. A **101**, 053619 (2020).
[36] E. V. H. Doggen and J. J. Kinnunen, Phys. Rev. Lett. **111**, 025302 (2013).
[37] T. Shi, E. Demler, and J. I. Cirac, Ann. Phys. **390**, 245 (2018).
[38] T. D. Lee, F. E. Low, and D. Pines, Phys. Rev. **90**, 297 (1953).
[39] E. H. Lieb and F. Y. Wu, Phys. Rev. Lett. **20**, 1445 (1968).
[40] U. Schollwöck, Ann. Phys. **326**, 96 (2011).
[41] S. Bour, D. Lee, H.-W. Hammer, and Ulf-G. Meißner, Phys. Rev. Lett. **115**, 185301 (2015).
[42] B. Kain and H. Y. Ling, Phys. Rev. A **96**, 033627 (2017).
[43] L. Hackl, T. Guaita, T. Shi, J. Haegeman, E. Demler, and J. I. Cirac, arXiv:2004.01015v2.
[44] G.-S. Tian, Phys. Lett. A **228**, 383 (1997).
[45] M. Köhl, APS March Meeting, 2012 (unpublished).
[46] C.-L. Hung, X. Zhang, L.-C. Ha, S.-K. Tung, N. Gemelke, and C. Chin, New J. Phys. **13**, 075019 (2011).
[47] G. Veeravalli, E. Kuhnle, P. Dyke, and C. J. Vale, Phys. Rev. Lett. **101**, 250403 (2008).
[48] S. Manz, R. Bücker, T. Betz, Ch. Koller, S. Hofferberth, I. E. Mazets, A. Imambekov, E. Demler, A. Perrin, J. Schmiedmayer, and T. Schumm, Phys. Rev. A **81**, 031610(R) (2010).
[49] J.-Y. Choi, S. W. Seo, W. J. Kwon, and Y.-i. Shin, Phys. Rev. Lett. **109**, 125301 (2012).
[50] F. Scazza, G. Valtolina, P. Massignan, A. Recati, A. Amico, A. Burchianti, C. Fort, M. Inguscio, M. Zaccanti, and G. Roati, Phys. Rev. Lett. **118**, 083602 (2017).
[51] S. Bravyi and D. Gosset, Commun. Math. Phys. **356**, 451 (2017).